Available online at www.sciencedirect.com
SCIENCE DIRECT
Polymer 46 (2005) 6243–6249
polymer
www.elsevier.com/locate/polymer

Preparation and properties of polypropylene/org-attapulgite nanocomposites

Lihua Wang[a,b], Jing Sheng[a,*]

[a]School of Materials Science and Engineering, Tianjin University, Tianjin 300072, China
[b]Department of Chemical Engineering, Tsinghua University, Beijing 10084, China

Received 15 October 2004; received in revised form 15 April 2005; accepted 17 May 2005
Available online 14 June 2005

Abstract

Polypropylene (PP)/org-attapulgite (ATP) nanocomposites were prepared by melt blending in a mixer apparatus. Org-attapulgite was attained by silane coupling agent modification first and then graft-polymerization with butyl acrylate. Scanning electron microscopy (SEM) and transmission electron microscopy (TEM) were used to assess the clay morphology and the dispersion of the org-attapulgite, respectively. The changes of crystalline structure for PP nanocomposites were characterized by X-ray diffraction (XRD). The mechanical properties of PP/attapulgite nanocomposites were studied through tensile and impact tests. The thermal and dynamic mechanical properties were characterized by differential scanning calorimetry (DSC) and dynamic mechanical analysis (DMA). The strength and stiffness of PP/org-ATP nanocomposites were both improved significantly in the presence of organic attapulgite. In addition, the incorporation of org-ATP also gave rise to an increase of the storage modulus and the changes of the glass transition temperature for PP composites. TEM and XRD results revealed the addition of attapulgite did not change the crystal structure of PP, however org-attapulgite acted as nucleating agents for the crystallization of PP.

Keywords: Polypropylene; Attpulgite; Nanocomposites

1. Introduction

In recent years, organic–inorganic nanometer composites have attracted great interest, both in industry and in academia, because they often exhibit remarkable improvement in mechanical and other properties when compared with plain polymer or conventional micro and macro-composites, such as high modulus, increased strength and heat resistance [1–4]. For example, polymer/montmorillonite (MMT) nanocomposites, such as PA6/MMT [5], PET/MMT [6], PEO/MMT [7], PMMA/MMT [8–9], have successfully been prepared by many researchers. This is because they can intercalate MMT layers and finally form intercalated or exfoliated nanocomposites. However, for polyolefin polymers, such as PP and PE, which do not include any polar group in their backbone, silicate layers even modified by nonpolar long alkyl groups are polar and incompatible with polyolefin. Generally, there are two major methods to prepare PP/clay nanocomposites [10]: (1) polar functional oligomer as a comptabilizer. (2) Clay is pre-dispersed in the polymer compatible to PP. The main purpose for above two methods is to improve interfacial interaction. As a result, the properties of nanocomposites are strongly influenced by the nature of filler/matrix interface. Of course, surface modification of nano-fillers is also very important for the nanocomposites. In general, there are two ways to modify the surface of inorganic particulates [11]. The first one is carried out through surface absorption or reaction with small molecules, such as silane coupling agent. The second method is based on grafting polymeric molecules through covalent bonding to the hydroxyl groups existing on the particles. In our studies, another clay that is different from MMT, attapulgite, is adopted and filled in the PP matrix. Attapulgite (or palygorskite-as it often called) is a crystalline hydrated magnesium aluminum silicate with unique three-dimensional structure and has a fibrous morphology. Attapulgite has the structural formula

* Corresponding author. Tel.: +86 22 2740 6647; fax: +86 22 2740 4724.
E-mail address: shengxu@public.tpt.tj.cn (J. Sheng).

0032-3861/$ - see front matter © 2005 Elsevier Ltd. All rights reserved.
doi:10.1016/j.polymer.2005.05.067

$Si_8O_{20}Mg_5(Al)(OH)_2(H_2O)_4 \cdot 4H_2O$, and its ideal structure is studied by Bradley early in 1940 and shown in Fig. 1 [12].

The distinguishing feature of its structure is that the Si–O tetrahedra form long strips, each an amphibole unit wide, on alternate sides of the oxygen sheet in a manner which confers a regular corrugated Si–O structure [13]. The formulas are written as such to indicate the two types of water present, magnesium coordinated water and adsorbed water. The structure of the mineral results in zeolite-like channels, which are approximately 3.7×6.0 and 5.6×11.0 Å wide, respectively [14]. These channels may be filled with water or organic molecules. Specific surface areas of about 200 m^2/g may, therefore, result from fine particle size rather than significant contributions from internal channel surface. Because of its structural morphology, attapulgite has received considerable attention with regard to the adsorption of organics on the clay surface, but there is only a little report about its use in the nanocomposites.

In our pervious work [15], the surface modification of attapulgite in making nanocomposites was suggested. In this study, we report a new kind of PP/clay nanocomposites and a new method to prepare the nanocomposites by melt blending, using organo-attapulgite modified by silane coupling agent first and next grafting polymerization with poly(butyl acrylate) instead of maleic anhydride-modified PP. The strong interaction caused by the grafting reaction can improve the dispersion effect of the attapulgite in the PP matrix. The corresponding properties of the resulting nanocomposites were investigated.

2. Experiment

2.1. Materials

PP (grade1300, melt index 1.325 g/10 min) used in this study was purchased from Beijing Yanshan Petrochemical Co, Ltd; China.

Attapulgite(ATP) clay was obtained from Hongqing Limited Company (Xuyi, Jiangsu, China) (200-mesh sieve, specific surface area 150 m^2/g).

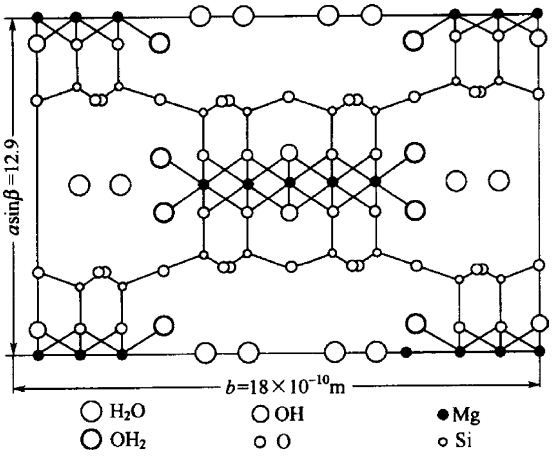

Fig. 1. Crystalline structure of attapulgite from (001) plane.

The γ-methacryloxypropyl trimethoxysilane(KH-570), utilized as the coupling agent, was purchased from Shanghai Yaohua Chemical Reagent Company, Shanghai, China. Butyl acrylate (BA), toluene and benzoyl peroxide (BPO) were all analytical grade.

2.2. Preparation of organophilic attapulgite

KH-570 hydrolysis was performed under acidic conditions using a mixture of KH-570 in a water solution of isopropyl alcohol. Surface treatment was carried out under nitrogen atmosphere in dry toluene at 50–60 °C. Grafting of ATP/KH-570 (OATP) with BA was achieved by dispersing the KH-570 modified ATP in toluene. Then, an appropriate amount of butyl acrylate was added to the mixture under nitrogen atmosphere with vigorous stirring. The sample was heated to 60 °C, and a radical initiator, BPO, was added to the mixture. Finally the mixture was heated to 80–90 °C for 10 h. The products were filtered and washed with toluene for three times. Obtained hybrid org-ATP (BOATP) was dried at 120 °C under vacuum.

2.3. Preparation of PP/clay nanocomposites (PPCN)

The dried BOATP was melt-blended with PP in a mixer apparatus(XXS-30) mixer, China) at a temperature of 185 °C with a residence time of 10 min at 32 rpm to obtain PPCN. The BOATP contents were varied from 1 to 7% by weight. The obtained composites were compression molded at 190 °C in a parallel plate press for 10 min. Specimens about 1 mm in thickness were cut from the plaques for the different measurements realized in the present study.

2.4. Microscopic examination (SEM and TEM)

The morphology of the ATP, OATP and BOATP were inspected in a scanning electron microscope (SEM) named PHILIPS XL-30. Powder samples were dispersed in ethanol in an ultrasonic bath for 10 min before the SEM examination. Transmission electron microscopy (TEM) observations of an ultrathin sections of the PP nanocomposites were carried out with a PHILIPS EM 400ST instrument with an acceleration voltage of 200 kV. The ultrathin samples were the made with a microtome.

2.5. X-ray diffraction (XRD)

Wide-angle X-ray spectra were recorded with a Ragaku Model D/max-2500 diffractometer; the X-ray beam was nickel-filtered Cu Kα ($\lambda = 0.1542$ nm) radiation operated at 40 kV and 100 mA; corresponding data were collected from 3 to 60° at a scanning rate of 1°/min.

2.6. Mechanical properties

Tensile test was carried out using a Testometric M350-20KN tester with a speed of 10 mm/min at room temperature. E-modulus, tensile strength and elongation at break were evaluated from stress–strain data. The notched Izod impact strength was measured with CHARPY XCJ-40 according to the respective standards.

2.7. Dynamic mechanical analysis (DMA)

The dynamic mechanical analysis was performed using a Netzsch DMA 242 device. The testing was carried out in tension mode at 5 Hz in a broad temperature range from −150 to 190 °C in nitrogen atmosphere.

2.8. Thermal analysis (DSC)

The melting and crystallization behaviors of the nanocomposites were carried out with a Perkin–Elmer DSC-7 differential scanning calorimeter thermal analyzer. About 8 mg of polymer sample was sealed into aluminum pans. The temperature was raised from 30 to 200 °C at a rate of 10 °C/min under nitrogen atmosphere. The sample was kept for 10 min at this temperature to eliminate the heat history before cooling at 10 °C/min.

3. Results and discussion

3.1. Effect of surface modification on ATP

Fig. 2 shows the XRD patterns of ATP, OATP, and BOATP. The peaks at $2\theta = 8.3$, 13.6, 19.7, and 26.6° correspond to the primary diffraction of the (110), (200), (040), and (400) planes of the clay respectively. The results clearly show that the four-plane characteristic peaks for pure ATP and treated ATP do not change at all. That is to say, surface treatment of ATP has no evidently effects on its crystal structure. But from the results of FT-IR, XPS and DTA [15], the covalent bond has formed in OATP and BOATP.

SEM micrographs of ATP, OATP and BOATP are shown in Fig. 3. From Fig. 3 (a), we can see that the ATP has a fibrous morphology and its diameter is about 20 nm and length is 300–1000 nm. By way of surface modification using silane coupling agent, as shown in Fig. 3 (b), an average diameter of OATP is about 40 nm, and the small aggregates are still existent though the ultrasonic dispersion was adopted after surface modification. From the Fig. 3 (c), we can see the ATP clay re-aggregated when they were treated with the BA, the graft polymerization of BA may cause the BOATP to agglomerate.

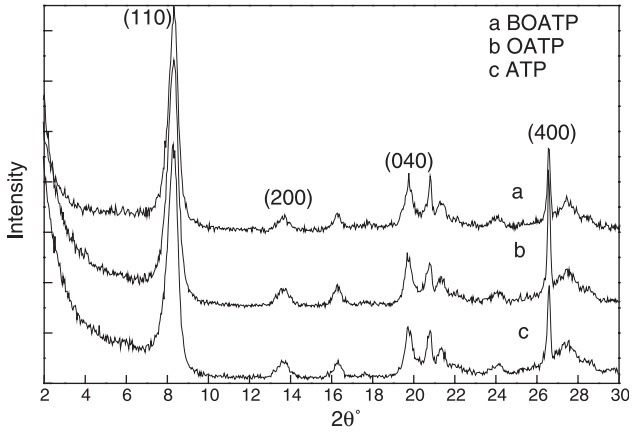

Fig. 2. XRD patterns of the clay.

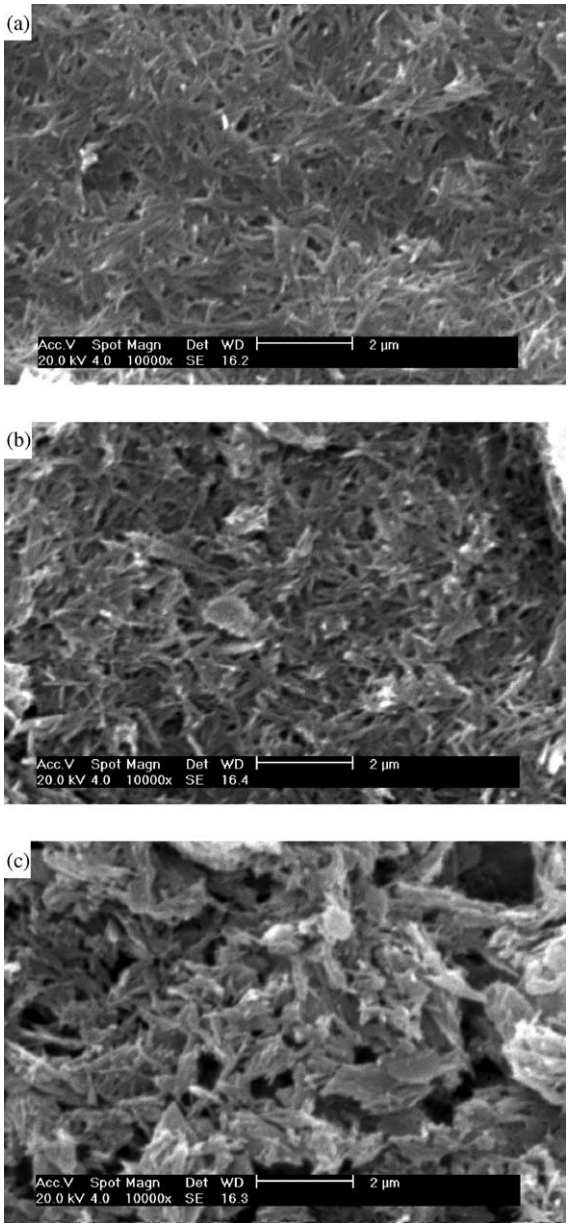

Fig. 3. SEM micrographs of (a) ATP (b) OATP and (c) BOATP.

3.2. The dispersion of BOATP in PPCN

It is known that the dispersion of a filler in the polymer matrix can have a significant effect on the mechanical properties of the composites. The dispersion of an inorganic filler in a thermoplastic is not an easy process. A good dispersion can be achieved by surface modification of the filler particles and appropriate processing conditions. The dispersibility of org-ATP in the PP matrix is confirmed by TEM shown in Fig. 4, where the dark parts are Org-ATP and their diameter is about 40 nm. In the case of nanocomposites containing 5 wt% org-ATP, most ATP aggregates are broken down to primary particles. This should maximize the interfacial interaction between the nanoparticles and the polymer. However, some aggregates are still found in the PP matrix, which may have an unfavourable effect on the mechanical properties.

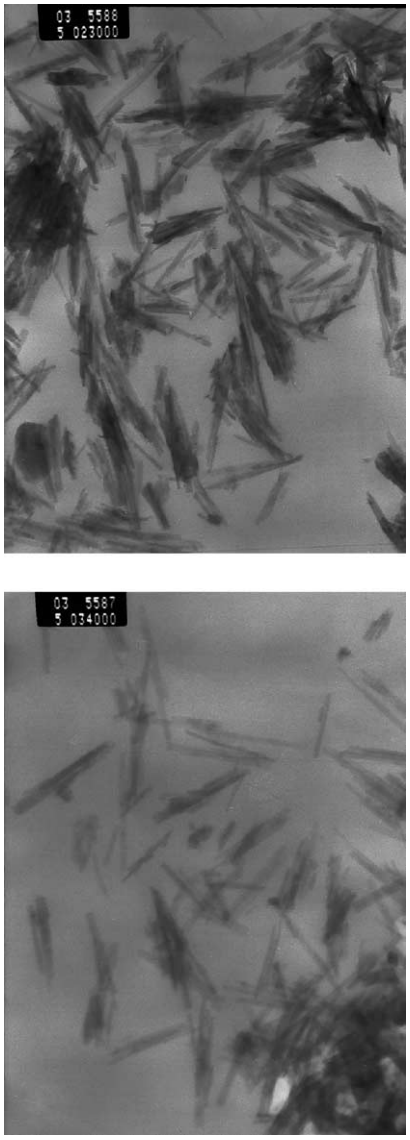

Fig. 4. TEM micrographs of the nanocomposites with 5 wt% filler.

3.3. Crystal structure and crystallization behavior of PPCN

Fig. 5 shows the XRD patters of the PP and PPCN. As shown in the figure, pure PP shows five prominent peaks in the 2θ range of 10–30°, which correspond to monoclinic α crystalline phase [16]. In the case of PPCN composites, same numbers of peaks are observed in the range of 2θ, which suggests that these also contain mainly α-phase. However, the difference lies in the relative intensities of the peaks, especially the intensity of peak 2 (040 reflection of α-phase of PP), which change considerably in the presence of nanoparticles. From the curve of PPCN, we did not find the β-phase crystal of PP which diffraction peak at $2\theta = 16.5°$ corresponds to the (300) plane. This indicates that the addition of clay does not affect the crystal structure of the PP matrix in this case. The mechanical properties of the nanocomposites can be significantly changed if the crystallization characteristics of PP have been altered. Fig. 6 presents the DSC cooling scan thermograms of pure PP and PP nanocomposites. The crystallization temperature of pure PP is 109.8 °C; while 3 wt% BOATP addition increases this temperature up to 116.8 °C. The DSC results clearly show that the addition of a small amount of clay into the PP matrix leads to an increase of crystallization temperature of polymer matrix, implying that the ATP clay act as efficient nucleating agents for the crystallization of PP matrix. From our previous study of isothermal crystallization kinetics for PPCN nanocomposites [17], we have proved the above conclusions.

3.4. Mechanical properties of PPCN composites

The mechanical properties of PPCN nanocomposites are measured and shown in Figs. 7–9. The tensile strength (Fig. 7) of composites prepared in the presence of original ATP decreased with increasing ATP content. In the presence of BOATP, yield stress increased with increasing clay content from 0 to 3 wt% and 13% improvement is obtained in PP/BOATP (3 wt%)compared with pure PP. As

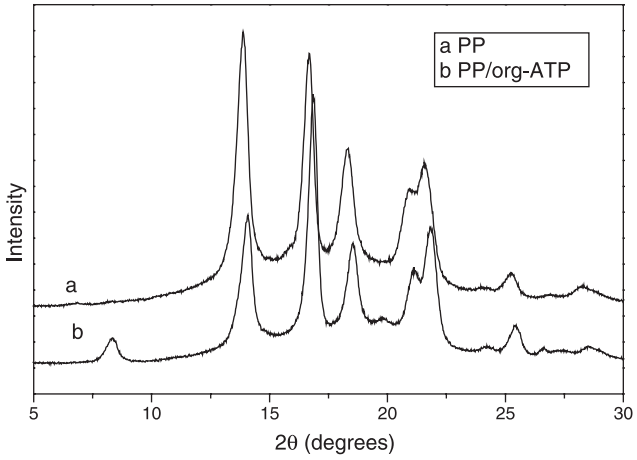

Fig. 5. XRD spectra for the PP and PP/org-ATP nanocomposites.

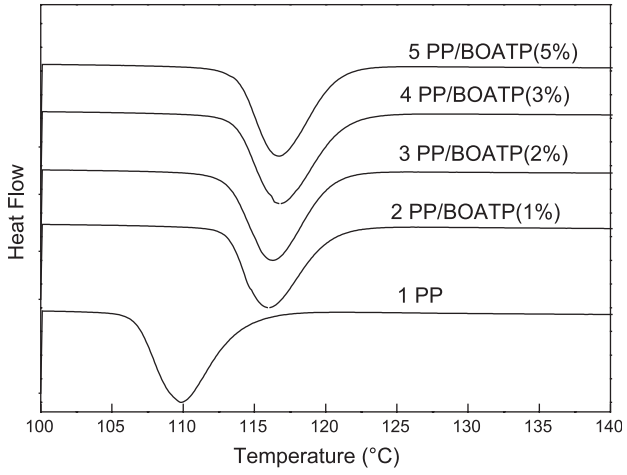

Fig. 6. DSC cooling scan thermograms of PP and its nanocomposites.

shown in Fig. 8, all samples showed an increased modulus with increasing clay content. However, the improvement range for PP/BOATP is larger than that of PP/ATP. These results suggest that the utilization of surface modification agent is essential to achieve higher stiffness. The notched Izod impact strength of composites was also affected by the organo-attapulgite content. As shown in Fig. 9, the toughness increased with increasing org-ATP content to 3 wt% and 70% improvement than pure PP. In the absence of surface modification agent, the notched Izod impact strength was up to 20% higher than that of the bulk polymer. This suggests the nanometeric dispersion of attapulgite clay in polymer matrix leads to improved modulus and strength.

3.5. Dynamic mechanical properties (DMA)

DMA is often used to study relaxation in polymers. An analysis of the storage modulus, loss modulus, and tan δ curves is very useful in ascertaining the performance of samples under stress and temperature. McGrum and colleagues [18] have demonstrated that the tan δ curve of PP exhibits three relaxations localized in the vicinity of

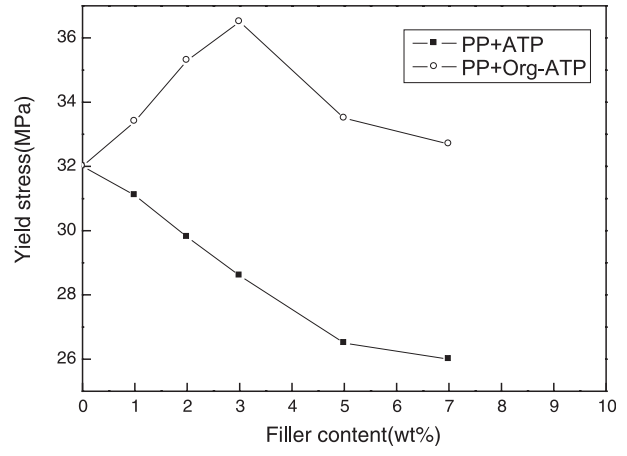

Fig. 7. Effect of clay loading on tensile strength of PP nanocomposites.

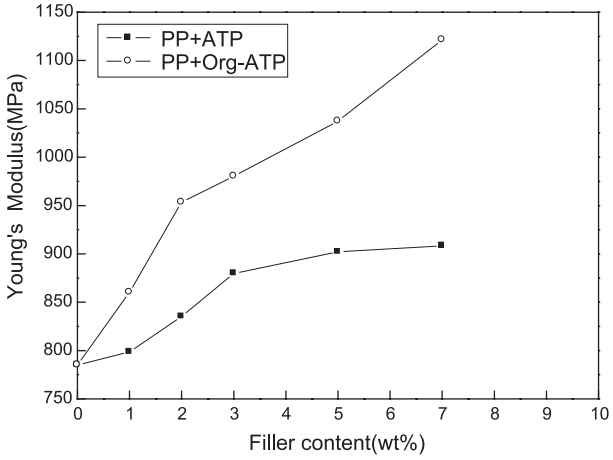

Fig. 8. Effect of clay loading on Young's modulus of PP nanocomposites.

−80 °C (γ), 100 °C (α) and at 10 °C (β). In the present work, the study was focused on the β-relaxation of PP that corresponds to the glass-rubber transition of the amorphous portions and the temperature of the maximum peak is assigned to the glass transition temperature (T_g). The glass transition temperature can be defined as the maximum of the transition in the loss modulus curve or in the loss tangent curve.

Fig. 10 shows the dynamic storage modulus E' and loss factor tan δ as a function of temperature for PP and composites. The results from Fig. 10(a) show that the storage modulus of the composites are higher than that of pure PP, which indicating that the incorporation of BOATP into PP matrix remarkably enhances stiffness and has a good reinforcing effect. But the Young's modulus (Fig. 8) are contract to the storage modulus (Fig. 10). We think the main reason may be the dispersion uniformity of the BOATP in the matrix of PP. At higher content, aggregation of the BOATP may take place. As a consequence, the repeatability of the mechanical properties results is not very good. Fig. 10(b) reveals the effect of clay on the loss factor (tan δ)

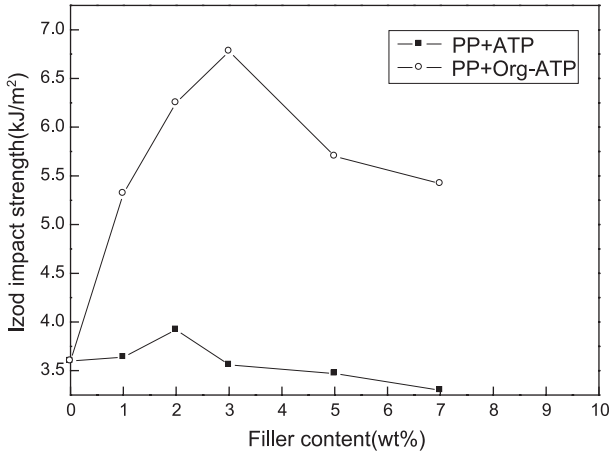

Fig. 9. Effect of clay loading on notched Izod impact strength of PP nanocomposites.

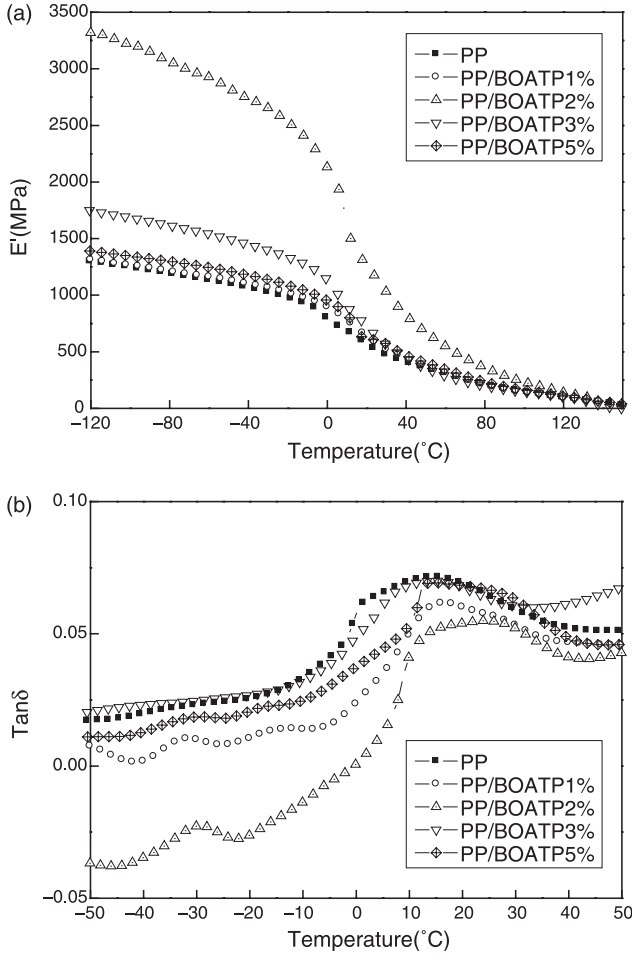

Fig. 10. (a) E' of pure PP and its composites as a function of temperature. (b) tan δ of pure PP and its composites as a function of temperature.

for PPCN composites. The glass transition temperatures of PPCN composites, which can be derived from curves of log tan $\delta - T$, are lower than that of pure PP in general other than the 2 wt% ATP loading. It is well known that the T_g of a polymer depends on the mobility of the chain segment of the macromolecules in the polymer matrix. If the molecular chain is restricted, motion or relaxation of the chain segment becomes difficult at the original glass transition temperature and becomes easy at higher temperature. The T_g and the tan δ values at T_g peak, -20 and 25 °C are reported in Table 1. In addition, to evaluate the effect of clay loading on mechanical properties of PP, the storage modulus of the studied composites at -20 and 25 °C are also represented in Table 1. As shown in Table 1, the PPCN composites exhibited a higher storage modulus than the pure PP over the more board temperature range. When the content of BOATP is 2 wt%, the values of E' are two times or higher than that of PP. However, the value of T_g is higher than the pure PP. This conclusion seems to conflict with the results of Fig. 7, the major factors may be related to the degree of particle homogeneous dispersion in the polymer matrix and the interactions between the filler and the polymer. The mechanism of how the addition of clay affects the T_g of PPCN needs to be studied further.

Table 1
Dynamic mechanical properties of PP and its composites at 5 Hz

Materials	E' (MPa)/tan δ at 5 Hz		T_g (°C)/tan δ at peak 5 Hz
	-20 °C	25 °C	
PP	980/0.0253	513/0.0641	18.5/0.072
PP/BOATP1%	1021/0.0104	562/0.0560	17.6/0.062
PP/BOATP2%	2533/0.0262	1128/0.0538	21.3/0.055
PP/BOATP3%	1341/0.0267	630/0.0631	18.0/0.074
PP/BOATP5%	1091/0.0204	598/0.0665	15.7/0.069

4. Conclusion

A new kind of organophilic clay, attapulgite, was used in this study modified by silane agent and butyl acrylate. The PP nanocomposites with the clay were prepared by melt blending. The surface grafting reaction improved the dispersion effect of attapulgite in PP matrix but had no effect on its crystal structure. The mechanical properties of PP nanocomposites were improved by the addition of attapulgite. In addition, the incorporation of organophilic attapulgite also gave rise to a considerable increase of the storage modulus and a decrease of the tan δ value demonstrating the reinforcing effect of clay on the PP matrix. The glass transition temperature decreased slightly in the presence of attapulgite other than 2 wt% clay loading. The thermal analysis reveals that the attapulgite nanoparticles are an effective nucleating agent and accelerated the crystallization process considerably.

References

[1] Hu X, Zhao XY. Polymer 2004;45(11):3819–25.
[2] Kawasumi M, Hasegawa N, Kato M, Okada A. Macromolecules 1997;30(20):6333–8.
[3] Le Baron PC, Wang Z, Pinnavaia TJ. Appl Clay Sci 1999;15(1-2):11–29.
[4] Lee HS, Fishman D, Kim B, Weiss RA. Polymer 2004;45(23):7807–11.
[5] Fornes TD, Paul DR. Polymer 2003;44(17):4993–5013.
[6] Lee SR, Park HM, Lim H, Kang T, Li XC, Cho WJ, et al. Polymer 2002;43(8):2495–500.
[7] Liao B, Song M, Liang H, Pang Y. Polymer 2001;42(25):10007–11.
[8] Okamoto M, Morita S, Taguchi H, Kim YH, Kotato T, Tateyama H. Polymer 2000;41(10):3887–90.
[9] Yasutaka M, Reiko S. Polymer 2004;45(1):95–100.
[10] Liu XH, Wu QJ. Polymer 2001;42(25):10013–9.
[11] Rong MZ, Ji QL, Zhang MQ, Friedrich K. Eur Polym J 2002;38(8):1573–82.
[12] Bradley WF. Am Miner 1940;25(6):405–10.
[13] Cao E, Bryant R, Williams DJA. J Colloid Interf Sci 1996;179(1):143–50.

[14] Frost RL, Cash GA, Kloprogge TJ. Vib Spectrosc 1998;16(1):173–84.
[15] Wang LH, Sheng J. J Macrom Sci, Pure Appl Chem 2003;40A(11): 1135–46.
[16] Saujanya C, Radharkishnan S. Polymer 2001;42(16):6723–31.
[17] Wang LH, Sheng J, Wu SZ. J Macromol Sci Phys 2004;43B(5): 935–46.
[18] McGrum NG, Read BE, Williams G. Anelastic and dielectric effects in polymeric solids. London. London: Wiley; 1967.